

SPHERICALLY SYMMETRIC NLTE MODEL ATMOSPHERES OF HOT HYDROGEN-HELIUM FIRST STARS

JIŘÍ KUBÁT

Astronomický ústav, Akademie věd České republiky, CZ-251 65 Ondřejov, Czech Republic
Draft version October 1, 2012

ABSTRACT

We present results of our calculations of NLTE model stellar atmospheres for hot Population III stars composed of hydrogen and helium. We use our own computer code for calculation of spherically symmetric NLTE model atmospheres in hydrostatic and radiative equilibrium. The model atmospheres are then used for calculation of emergent fluxes. These fluxes serve for the evaluation of the flow of high-energy photons for energies higher than ionization energies of hydrogen and helium, the so-called ionizing photon fluxes. We also present the time evolution of the ionizing photon fluxes.

Subject headings: Stars: atmospheres – radiative transfer – stars: Population III – first stars

1. INTRODUCTION

At the beginning of the era of modern NLTE stellar atmosphere modelling at the early 70's, the chemical composition of computed model atmospheres had to be as simple as possible to enable their calculation at computers that were available at that time. Therefore, these models included only minimum number of elements, selected according to their importance for the atmospheric structure properties. First models were purely hydrogen (Auer & Mihalas 1969, 1970), later also helium was included (Mihalas & Auer 1970; Auer & Mihalas 1972; Kudritzki 1973, 1976) to calculations. Due to computer limitations, the absorption by heavier elements was not considered, and, of course, also the absorption by a huge number of metal lines in the ultraviolet spectral region was omitted. These metal lines cause lowering the ultraviolet flux and enhancing the flux in the visual region. This important effect is known as line blanketing (see, e.g., Mihalas 1978). Great effort (started by Anderson 1985, 1989) was necessary to include the line blanketing into NLTE model atmospheres calculations, and nowadays it is possible to calculate NLTE model atmospheres with this effect taken into account properly. One of the most widely used codes for calculation of static NLTE line blanketed plane-parallel model atmospheres is the code TLUSTY (Hubeny 1988; Hubeny & Lanz 1995). NLTE line-blanketing can be also treated by other model atmosphere codes, like the model atmosphere package TMAP (Werner et al. 2003). For the case of NLTE moving atmospheres with line blanketing, codes CMFGEN (Hillier & Miller 1998), PHOENIX (e.g. Hauschildt et al. 1997), FASTWIND (Santolaya-Rey et al. 1997; Puls et al. 2005), and WMBasic (e.g. Pauldrach 2003, and references therein) are available.

All these mentioned model atmosphere codes were developed and used with the primary objective to reproduce the observed emergent radiation from hot stars. The hydrogen-helium static model atmospheres calculated by Auer & Mihalas served only as a first approximation of NLTE hot stellar atmosphere modelling. However, there is a group of stars, whose chemical composition corresponds exactly to what was calculated by Auer & Mihalas in the early 70's, namely the first stars in the Universe. Since the Universe at its beginning was

practically free of metals and consisted only of hydrogen, helium, and a very little amount of lithium (see, e.g., reviews of Bromm & Larson 2004; Johnson et al. 2008; Bromm et al. 2009), the first stars may be safely assumed to consist only of hydrogen and helium, since the influence of lithium on the stellar atmospheric structure is negligible.

Thus, in order to obtain model atmospheres of first stars, it is simply sufficient to use the first codes for calculation of NLTE model atmospheres from the early 70's, or to repeat such calculations with contemporary sophisticated model atmosphere codes and just to skip metals from the calculations. The latter was done by Tumlinson & Shull (2000), who used the code TLUSTY to calculate simple hydrogen-helium model atmospheres and rediscovered that “*A model atmosphere is necessary because a simple blackbody curve for each T_{eff} will not accurately reproduce the spectrum ...*” (cf. Unsöld 1955, where the history of the finding that the stellar radiation is not the blackbody one is thoroughly described). They concluded that neglecting all the metal opacities leads to enhancement of the UV flux emerging from the model stellar atmosphere, a fact that was well known before, but in opposite formulation, namely that adding metallic opacity reduces the ultraviolet stellar flux.

The presence of high UV flux emerging from the hydrogen-helium model atmospheres describes an important source of radiation, which is able to ionize the intergalactic medium in the early Universe evolution (Venkatesan et al. 2003). Indeed, high fluxes at high frequencies caused by missing stellar opacity in those spectral regions are extremely important in cosmology (Venkatesan & Truran 2003). Model atmospheres of first stars and their influence on ionizing radiation were also studied in detail by Schaerer (2002, 2003).

The absence of metals in the atmospheres of first stars has an additional effect. Since the winds of hot stars are driven by radiation scattered by spectral lines, there was a question whether the first stars have stellar winds. Existence or non-existence of the stellar wind has dramatic influence on the first star evolution. Bromm, Kudritzki, & Loeb (2001) calculated unified model atmospheres (using an improved version of the method of Santolaya-Rey et al. 1997) and did not find any effect of the velocity field on line profiles for low

mass-loss rates. Kudritzki (2002) tested the existence of winds of first stars by calculating wind models using the depth dependent line force multiplier parameters k , α , and δ . He tried to mimic the zero metallicity of the first stars using a method, which implicitly assumes driving of the wind by metallic lines. He pointed out the possibility of multicomponent effects in the wind of first stars. These were later studied in detail by Krtićka et al. (2003, 2010). However, the principal question of existence or non-existence of the winds of first stars deserved more detailed study. The code of Krtićka & Kubát (2004) enabled calculation of the radiative force directly using actual level populations and opacities of individual elements at each depth point, without the necessity to introduce parameterization of the radiative force by means of the line force multipliers. Consequently, this method gives implicitly depth-dependent line force and allows to include consistently any chemical composition. Using this code, Krtićka & Kubát (2006, 2009) studied stellar winds of first stars and confirmed the fact found by Kudritzki (2002) that the first stars have extremely weak winds. These calculations also showed that using static approximation for calculation of model atmospheres of first stars is adequate. For these calculations, which were done using the core-halo approximation, it was necessary to determine the flux at the lower boundary of the wind region. To this end, the emergent radiation from the static spherically symmetric NLTE model atmospheres was used. Consequently, Krtićka & Kubát did not check if the plane-parallel approximation, which has been frequently used by others, is adequate for modelling the atmospheres of first stars. Since the NLTE atmospheric models used by Krtićka & Kubát have not been published anywhere in detail, in this paper we present an extended set of NLTE model atmospheres used for this purpose.

2. MODEL ATMOSPHERES

2.1. Validity of static approximation

For the case when the thickness of the atmosphere is small compared to the stellar radius, the plane-parallel approximation offers a good choice. This happens for dwarf stars with relatively high surface gravitational acceleration ($\log g \gtrsim 4$). However, small deviations from the plane-parallel approximation were found even for subdwarfs (Gruschinske & Kudritzki 1979). For the case of white dwarfs they were found only in cores of some strong lines and were usually very small (Kubát 1995).

On the other hand, for Population I and II stars with lower surface gravities, giants and supergiants, the atmosphere is more extended, and it can no longer be considered as thin with respect to the stellar radius. In such case a spherically symmetric approximation is more realistic than the plane-parallel one. However, due to a weaker gravitational force in the atmospheres of giants and supergiants, the radiation force may easily overcome gravity there and give rise to a stellar wind. Consequently, such atmosphere can not be considered as a static one. Winds in hot star atmospheres are driven by radiation force generated by momentum transfer from absorptions and scatterings in lines of heavy elements, with a help of the force generated by continuum transitions and electron scattering. Note that the force gen-

erated by continuum transitions and electron scattering alone is not sufficient to drive the wind.

The first stars in Universe were born from pure hydrogen-helium mixture with no heavier elements. Consequently, since the radiation force does not overcome gravity there, the line driven wind does not exist there (see Krtićka & Kubát 2006, 2009) and atmospheres of these stars may be described using static approximation in both plane-parallel and spherically symmetric geometry.

2.2. Method of calculation

Our method for calculation of NLTE model stellar atmospheres is based on an accelerated lambda iteration (ALI) method and has been described in some detail in Kubát (1994, 1996, 1997b, 2001) and summarized in Kubát (2003). Using our code we calculated a grid of hydrogen-helium spherically symmetric NLTE model atmospheres in hydrostatic and radiative equilibrium. The helium abundance $Y_{\text{He}} = n_{\text{He}}/n_{\text{H}} = 0.1$. We considered a 16 level hydrogen atom (15 levels of H I + 1 level of H II) and a 50 level helium model atom (29 levels of He I + 20 levels of He II + 1 level of He III). Individual hydrogen levels correspond to main quantum numbers $n = 1, \dots, 15$. For He I, all levels up to $n = 4$ were taken separately according to orbital quantum number l , for $5 \leq n \leq 9$ we took 2 averaged levels for each n , one for singlets, one for triplets. The levels of He II were considered similarly as the hydrogen levels, however for $n = 1, \dots, 20$. Details of the model atoms used (oscillator strengths, photoionization cross sections, collisional excitation and ionization rates, line profiles) can be found in Kubát et al. (1999).

For temperature structure determination we used a combination of three methods. At large depths below the stellar radius $R_* = r(\tau_R \approx 2/3)$ (τ_R is the Rosseland optical depth) it was the differential form of the radiative equilibrium equation, above the stellar radius the integral form of radiative equilibrium equation, and for outermost layers the electron thermal balance method was used (for details see Kubát 1996, 2001; Kubát et al. 1999).

3. RESULTS OF CALCULATIONS

3.1. Model atmosphere parameters

Basic parameters (luminosity L_* , mass M_* , and radius R_*) of the first stars are taken from evolutionary calculations. For the original calculations used in Krtićka & Kubát (2009) a limited set of model parameters (taken from Marigo et al. 2001) was used. In addition to them, here we extended the set by using additional parameters from Marigo et al., and we also used other sources of stellar parameters following from other evolutionary calculations. Values of masses of these stars are still matter of debate and they are different in different calculations (cf. different results obtained by evolutionary calculations of Yoon & Langer 2005 or Yoon et al. 2006, and Hirschi 2007).

First stars model atmospheres calculated by Schaerer (2002) cover stellar masses from $5 M_{\odot}$ up to extremely high masses of $1000 M_{\odot}$. He used the code TLUSTY for calculation of H-He model atmospheres for stars with $T_{\text{eff}} > 20000 \text{ K}$, for colder stars he adopted the Kurucz LTE model atmospheres with a very low metallicity.

TABLE 1

MODEL ATMOSPHERE PARAMETERS AND STELLAR IONIZING PHOTON FLUXES Q_i FOR SELECTED MODEL ATMOSPHERES OF FIRST STARS WITH PARAMETERS FROM SCHAERER (2002).

model	R_* [R_\odot]	M_* [M_\odot]	L [L_\odot]	T_{eff} [K]	$\log g$	$Q(\text{H I})$	$Q(\text{He I})$ [photons $\cdot \text{s}^{-1}$]	$Q(\text{He II})$
ds999	15.57	1000.	$2.780 \cdot 10^7$	106170	5.053	$1.25 \cdot 10^{50}$	$8.59 \cdot 10^{49}$	$4.81 \cdot 10^{49}$
ds500	10.41	500.	$1.276 \cdot 10^7$	106900	5.102	$5.66 \cdot 10^{49}$	$3.85 \cdot 10^{49}$	$2.08 \cdot 10^{49}$
ds400	9.09	400.	$9.638 \cdot 10^6$	106660	5.123	$4.39 \cdot 10^{49}$	$2.99 \cdot 10^{49}$	$1.61 \cdot 10^{49}$
ds300	8.28	300.	$6.592 \cdot 10^6$	101620	5.079	$3.12 \cdot 10^{49}$	$2.06 \cdot 10^{49}$	$1.04 \cdot 10^{49}$
ds200	6.48	200.	$3.750 \cdot 10^6$	99770	5.116	$1.84 \cdot 10^{49}$	$1.20 \cdot 10^{49}$	$5.75 \cdot 10^{48}$
ds120	4.81	120.	$1.750 \cdot 10^6$	95720	5.153	$9.02 \cdot 10^{48}$	$5.67 \cdot 10^{48}$	$2.47 \cdot 10^{48}$
ds080	3.60	80.	$8.851 \cdot 10^5$	93320	5.230	$4.71 \cdot 10^{48}$	$2.90 \cdot 10^{48}$	$1.17 \cdot 10^{48}$
ds060	3.12	60.	$5.188 \cdot 10^5$	87700	5.228	$2.87 \cdot 10^{48}$	$1.69 \cdot 10^{48}$	$6.03 \cdot 10^{47}$
ds040	2.71	40.	$2.630 \cdot 10^5$	79430	5.175	$1.48 \cdot 10^{48}$	$8.22 \cdot 10^{47}$	$2.56 \cdot 10^{47}$
ds025	1.85	25.	$7.762 \cdot 10^4$	70800	5.301	$4.27 \cdot 10^{47}$	$2.38 \cdot 10^{47}$	$6.44 \cdot 10^{46}$
ds015	1.47	15.	$2.109 \cdot 10^4$	57410	5.281	$1.07 \cdot 10^{47}$	$5.19 \cdot 10^{46}$	$1.17 \cdot 10^{46}$
ds009	1.36	9.	$5.117 \cdot 10^3$	41880	5.127	$1.79 \cdot 10^{46}$	$5.69 \cdot 10^{45}$	$9.95 \cdot 10^{44}$
ds005	1.20	5.	$7.413 \cdot 10^2$	27540	4.982	$6.07 \cdot 10^{43}$	$3.28 \cdot 10^{40}$	$1.65 \cdot 10^{37}$

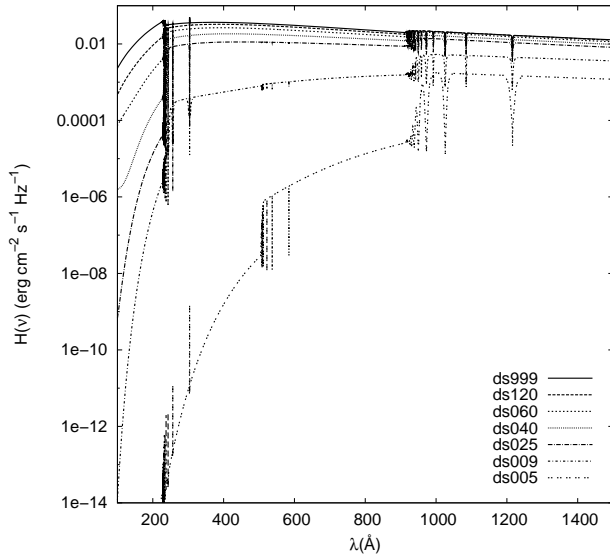


FIG. 1.— Plot of ultraviolet fluxes from selected model atmospheres of first stars with parameters from Schaerer (2002). Labels correspond to the first column of the Table 1.

We calculated spherically symmetric NLTE model atmospheres for parameters given in the Table 3 of Schaerer (2002), these parameters are listed here in the Table 1, corresponding temperature structures as a function of the column mass depth m are shown in the Figure A1. The column mass depth is related to the Rosseland optical depth by a relation

$$dm = (R_*^2/r^2)(\rho/\chi_R)d\tau_R, \quad (1)$$

where ρ is the density and χ_R the Rosseland opacity. All models display a rise of temperature in the outer parts of the atmosphere, where the strongest lines are optically thick and the continuum is optically thin. This is a typical NLTE effect in model atmospheres without metals (see, e.g. Auer & Mihalas 1970). In model atmospheres with metal line blanketing included, this temperature rise disappears (e.g., Lanz & Hubeny 2007).

To check the validity of the plane-parallel approximation for the first stars by direct comparison of spherically symmetric and plane-parallel models calculated with the same code (which has not been done yet), we also calculated NLTE plane-parallel model atmospheres for these

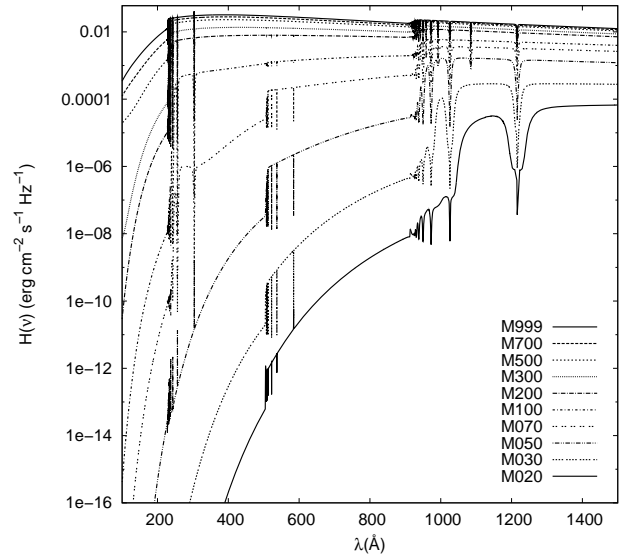


FIG. 2.— Plot of ultraviolet fluxes from selected model atmospheres of zero-age main sequence first stars from Marigo et al. (2001). Labels correspond to the first column of the Table 2.

stellar parameters. We found that the difference between the temperature structures of spherically symmetric and plane-parallel model atmospheres is relatively small, similarly to other cases where the atmospheric extension is not too large (cf. Gruschinske & Kudritzki 1979; Kubát 1996, 1997a,c, 1999). Also the difference between emergent fluxes from spherically symmetric and plane-parallel model atmospheres (the sphericity effect) is small, the flux from the spherically symmetric model atmosphere is slightly lower.

Although it was initially assumed that Population III stars should have very large masses of the order of hundreds M_\odot , Marigo et al. (2001) calculated an extensive grid of evolutionary models of Population III stars with masses $0.7 M_\odot \leq M \leq 100 M_\odot$ with the assumption of zero mass-loss.

For selected masses from this grid we calculated NLTE model atmospheres for models of stars with zero age. Their parameters (L_* , M_* , R_*) were taken from the on-line Table in Marigo et al. (2001) and are listed in the Table 2. Temperature structures for selected models are plotted in the Figure A2. All models display the same

TABLE 2
MODEL ATMOSPHERE PARAMETERS AND AND STELLAR IONIZING PHOTON FLUXES Q_i FOR SELECTED MODEL ATMOSPHERES FOR PARAMETERS FROM MARIGO ET AL. (2001).

model	R_* [R_\odot]	M_* [M_\odot]	L [L_\odot]	T_{eff} [K]	$\log g$	$Q(\text{H I})$	$Q(\text{He I})$ [photons $\cdot \text{s}^{-1}$]	$Q(\text{He II})$
M999	4.23	100	$1.282 \cdot 10^6$	94400	5.185	$6.74 \cdot 10^{48}$	$4.18 \cdot 10^{48}$	$1.74 \cdot 10^{48}$
M700	3.44	70	$6.871 \cdot 10^5$	89530	5.209	$3.72 \cdot 10^{48}$	$2.26 \cdot 10^{48}$	$8.31 \cdot 10^{47}$
M500	2.82	50	$3.597 \cdot 10^5$	84140	5.236	$2.01 \cdot 10^{48}$	$1.16 \cdot 10^{48}$	$3.80 \cdot 10^{47}$
M300	2.10	30	$1.189 \cdot 10^5$	73960	5.271	$6.61 \cdot 10^{47}$	$3.77 \cdot 10^{47}$	$1.05 \cdot 10^{47}$
M200	1.65	20	$4.456 \cdot 10^4$	65310	5.305	$2.40 \cdot 10^{47}$	$1.27 \cdot 10^{47}$	$3.24 \cdot 10^{46}$
M150	1.48	15	$2.128 \cdot 10^4$	57280	5.273	$1.08 \cdot 10^{47}$	$5.18 \cdot 10^{46}$	$1.16 \cdot 10^{46}$
M120	1.42	12	$1.132 \cdot 10^4$	49890	5.210	$5.00 \cdot 10^{46}$	$2.10 \cdot 10^{46}$	$4.04 \cdot 10^{45}$
M100	1.37	10	$6.653 \cdot 10^3$	44460	5.162	$2.48 \cdot 10^{46}$	$8.36 \cdot 10^{45}$	$1.39 \cdot 10^{45}$
M095	1.36	9.5	$5.727 \cdot 10^3$	43050	5.15	$1.99 \cdot 10^{46}$	$5.94 \cdot 10^{45}$	$9.92 \cdot 10^{44}$
M090	1.34	9	$4.875 \cdot 10^3$	41590	5.135	$1.55 \cdot 10^{46}$	$4.13 \cdot 10^{45}$	$6.71 \cdot 10^{44}$
M083	1.32	8.3	$3.810 \cdot 10^3$	39440	5.11	$1.03 \cdot 10^{46}$	$1.93 \cdot 10^{45}$	$2.49 \cdot 10^{44}$
M080	1.31	8	$3.412 \cdot 10^3$	38460	5.103	$8.34 \cdot 10^{45}$	$1.30 \cdot 10^{45}$	$1.60 \cdot 10^{44}$
M070	1.30	7	$2.234 \cdot 10^3$	34830	5.057	$2.90 \cdot 10^{45}$	$5.68 \cdot 10^{43}$	$2.14 \cdot 10^{42}$
M060	1.27	6	$1.426 \cdot 10^3$	31400	5.005	$5.73 \cdot 10^{44}$	$1.02 \cdot 10^{42}$	$8.98 \cdot 10^{38}$
M050	1.23	5	$8.054 \cdot 10^2$	27670	4.954	$7.23 \cdot 10^{43}$	$4.01 \cdot 10^{40}$	$1.93 \cdot 10^{37}$
M040	1.17	4	$3.837 \cdot 10^2$	23600	4.903	$8.65 \cdot 10^{42}$	$1.82 \cdot 10^{39}$	$1.47 \cdot 10^{35}$
M030	1.11	3	$1.476 \cdot 10^2$	19050	4.821	$5.71 \cdot 10^{41}$	$1.39 \cdot 10^{37}$	$4.75 \cdot 10^{31}$
M022	1.02	2.2	$4.497 \cdot 10^1$	14820	4.77	$2.07 \cdot 10^{40}$	$8.08 \cdot 10^{34}$	$1.44 \cdot 10^{28}$
M021	1.01	2.1	$3.767 \cdot 10^1$	14220	4.75	$9.83 \cdot 10^{39}$	$3.38 \cdot 10^{34}$	$3.16 \cdot 10^{27}$
M020	0.996	2	$3.133 \cdot 10^1$	13680	4.742	$6.69 \cdot 10^{39}$	$2.71 \cdot 10^{34}$	$1.68 \cdot 10^{27}$
M019	0.982	1.9	$2.552 \cdot 10^1$	13090	4.73	$3.67 \cdot 10^{39}$	$1.91 \cdot 10^{34}$	$8.43 \cdot 10^{26}$
M018	0.980	1.8	$2.080 \cdot 10^1$	12440	4.71	$5.19 \cdot 10^{39}$	$3.89 \cdot 10^{34}$	$1.93 \cdot 10^{27}$
M017	0.959	1.7	$1.641 \cdot 10^1$	11860	4.70	$1.18 \cdot 10^{39}$	$1.03 \cdot 10^{34}$	$1.12 \cdot 10^{26}$
M016	0.944	1.6	$1.274 \cdot 10^1$	11220	4.69	$3.75 \cdot 10^{38}$	$4.10 \cdot 10^{32}$	$1.49 \cdot 10^{24}$
M015	0.932	1.5	$9.772 \cdot 10^0$	10570	4.68	$3.66 \cdot 10^{38}$	$4.00 \cdot 10^{32}$	$1.45 \cdot 10^{24}$

type of the rise of temperature as the models in the Figure A1.

3.2. Ionizing fluxes and their evolution

As an immediate by-product of the model atmosphere calculation we can obtain the amount of radiation escaping from the stellar photosphere. This radiation significantly influences the circumstellar matter and it may be the reason for stellar winds. Fluxes from model atmospheres listed in the Table 2 (see also Fig. A2) for selected parameters from the large set of Marigo et al. (2001) were used as a lower boundary condition in wind calculations by Krtićka & Kubát (2009) for analysis of the existence of stellar winds.

For the case of Population III stars, the amount of highly energetic emergent radiation is of extreme importance, because it influences the ionization state of interstellar and intergalactic matter (therefore this radiation is often referred to as the ionizing radiation) and, consequently, it is important for the cosmic evolution (Venkatesan & Truran 2003).

Ultraviolet emergent fluxes from model atmospheres selected from the lists in the Tables 1 and 2 are plotted in the Figures 1 and 2, respectively. It is evident that the hottest and most massive (and hence most luminous) stars provide maximum flux in the far-ultraviolet region, which is the extremely important spectral region for generation of the “ionizing flux”. Contribution to this flux from the low-massive zero-age main sequence first stars is several orders of magnitude weaker.

For all models we calculate the stellar ionising photon flux Q (in photons s^{-1}) as

$$Q = 4\pi R_*^2 \int_{\nu_{\text{ion}}}^{\infty} \frac{F_\nu}{h\nu} d\nu \quad (2)$$

(ν_{ion} is the ionization frequency of the particular ionization edge) for H I, He I, and He II ionization edges. The values of the stellar ionizing fluxes are listed in the Tables 1 and 2. Comparing our results with those calculated by Schaerer (2002) by a totally independent code (TLUSTY) we find a good agreement. This supports the conclusion that both Schaerer’s and our codes give correct results.

We also plot the dependence of the number of ionizing photons for H I, He I, and He II ionization edges on stellar luminosity in the Figure 3. As expected, the number of ionizing photons rises with the stellar luminosity, the rise is significantly steeper for $L \lesssim 3.5L_\odot$.

In addition, we studied the evolution of ionizing fluxes with the stellar evolution. For stellar masses $10 M_\odot$, $20 M_\odot$, $50 M_\odot$ and $1000 M_\odot$ we calculated model atmospheres for evolved Population III stars. Parameters of these models are listed in Tables B1 – B4.

The ultraviolet emergent fluxes of some of the calculated evolved model atmospheres for masses $100 M_\odot$ and $50 M_\odot$ are shown in the Figure 4. The latter figure shows that the high ionizing flux present at zero-age main sequence first stars decreases with their evolution, as the stellar effective temperature decreases.

In order to describe the changes of the ionizing flux with time quantitatively, we calculated for each model listed in Tables B1 – B4 the ionizing photon flux after the Eq. (2) for each ionization (H I, He I, He II), and we listed these numbers in corresponding tables. The changes of these fluxes with the stellar evolution are shown in Figure 5. The fluxes first rise within the magnitude order of the initial value, then after reaching the maximum value they quickly drop by several orders of magnitude. The maximum value flux depends on the stellar mass, it is

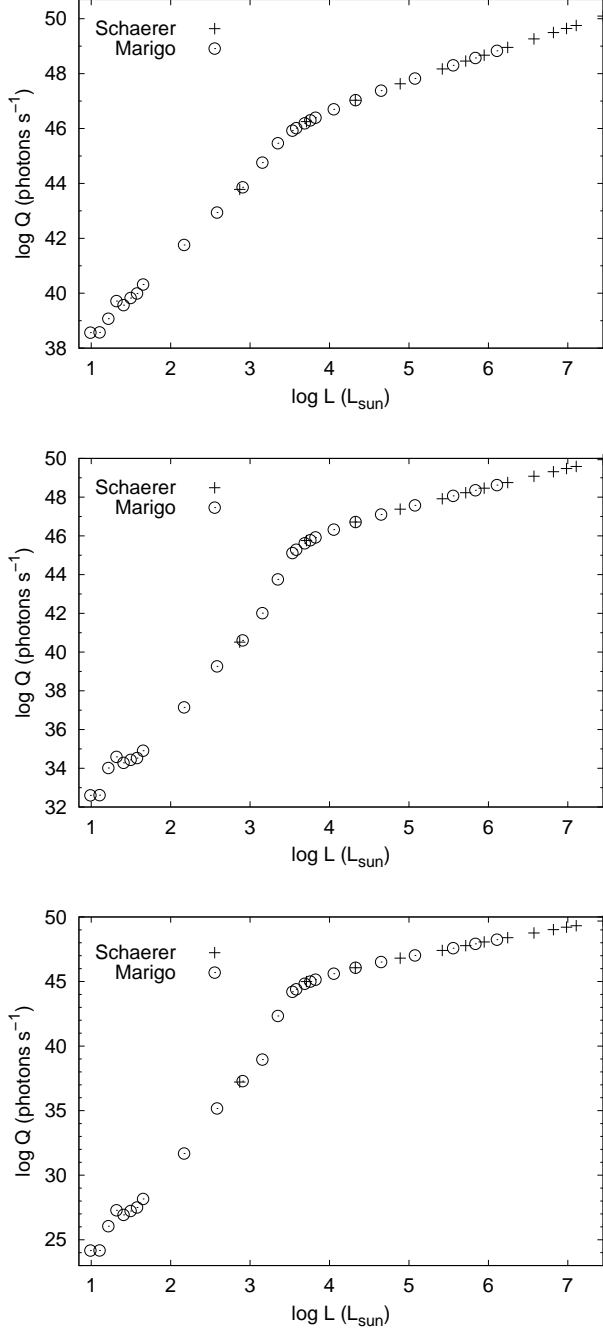


FIG. 3.— Number of ionizing photons Q as a function of the stellar luminosity for H I (upper panel), He I (middle panel), and He II (lower panel) continua. Stellar parameters are after Schaerer (2002, +) and Marigo et al. (2001, o).

reached sooner for more massive stars. The relative importance of first stars for the generation of ionizing photons at different ages is shown in the Fig. 6. The massive stars contribute by several orders of magnitude more, but since they evolve faster, their contribution lasts for much shorter time period than for stars with lower mass. For example, the $100 M_{\odot}$ star stops its contributing after $3 \cdot 10^6$ years, while the $10 M_{\odot}$ star contributes for about $19 \cdot 10^6$ years. However, the total contribution of the $10 M_{\odot}$ is smaller.

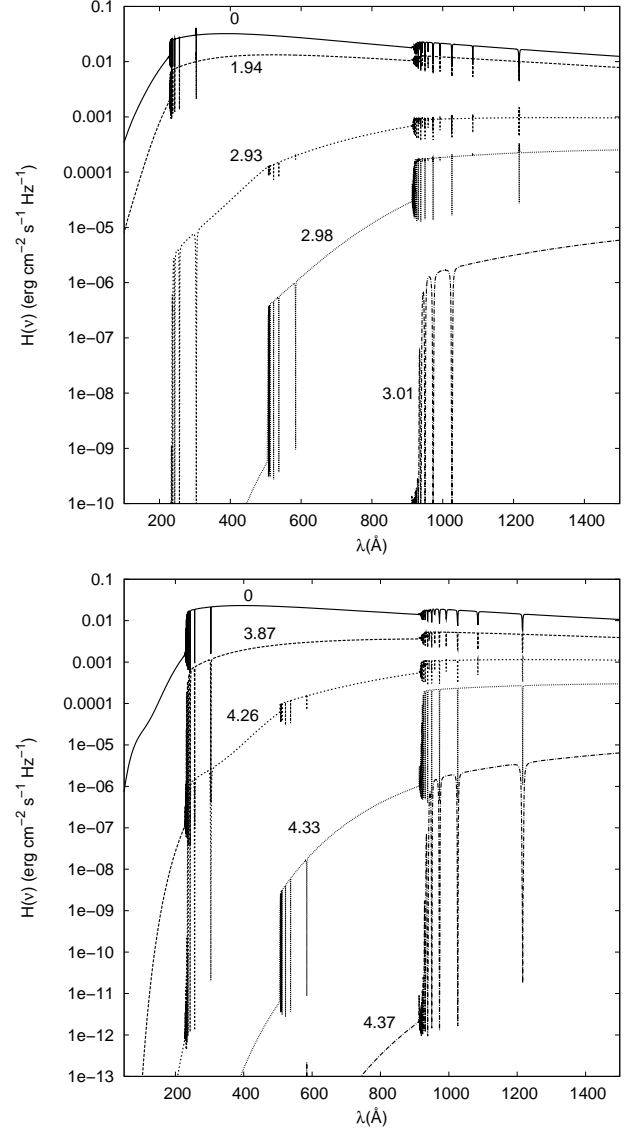


FIG. 4.— Plot of ionizing fluxes from selected model atmospheres after Marigo et al. (2001) for $100 M_{\odot}$ (upper panel) and $50 M_{\odot}$ (lower panel) for different ages of first stars with parameters given in Tables B1 – B4.. The curves are labeled with the stellar age in megayears.

4. CONCLUSIONS

We presented results of the NLTE model atmosphere calculations of first stars (Population III stars) assuming hydrogen-helium composition. These model atmospheres represent an extended set of model atmospheres used as a lower boundary flux condition in wind analyses of first stars by Krtićka & Kubát (2006, 2009). For the models we also calculated emergent fluxes and, in addition, the “ionizing photon fluxes”, which collect the contribution of the radiation in the ultraviolet part of the spectrum. Photon fluxes were calculated for radiation with shorter wavelength than H I, He I, and He II ionization edges. We also studied the time evolution of all three photon fluxes and we found strong dependence on the stellar mass, the more massive stars are more important contributors to ionizing photon flux. This underlines the importance of the question of the maximum stellar mass for zero age first stars.

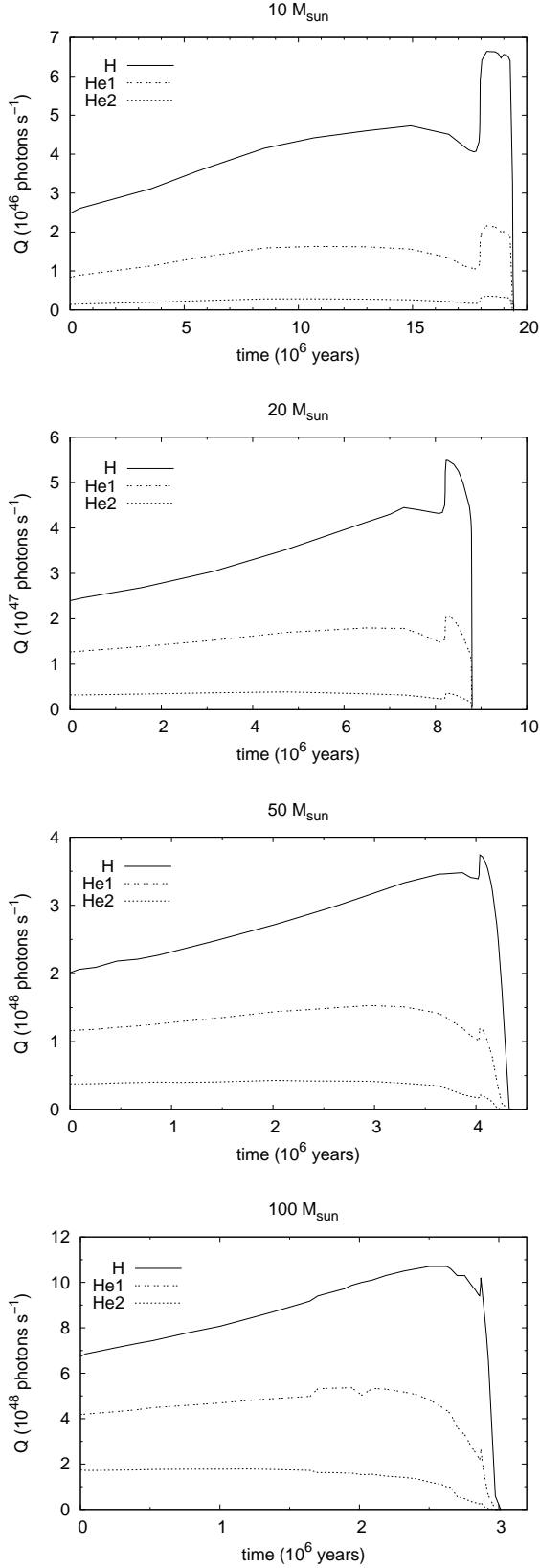


FIG. 5.— Number of ionizing photons Q (Eq. 2) in H I, He I, and He II continua as a function of time for different stellar masses ($10M_{\odot}$, $20M_{\odot}$, $50M_{\odot}$, $100M_{\odot}$) using evolutionary tracks from Marigo et al. (2001). The photon fluxes were calculated from model atmospheres calculated for parameters given in the Tables B1 – B4.

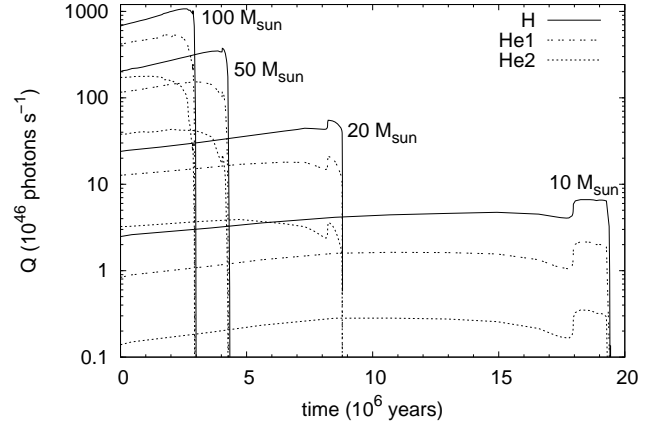


FIG. 6.— Comparison of the contribution to the ionizing photon flux from Population III stars with different masses. Model atmospheres are calculated after Marigo et al. (2001). The curves are labelled with the stellar mass. The same data as for Fig. 5 were used for this plot.

The author thanks Prof. Rolf-Peter Kudritzki for his comments to the manuscript. This research has made use of the NASA's Astrophysics Data System Abstract Service. This work was supported by a grant of the Grant Agency of the Czech Republic 205/08/0003. The Astronomical Institute Ondřejov is supported by the project RVO:67985815.

REFERENCES

- Anderson, L. S. 1985, *ApJ*, 298, 848
—, 1989, *ApJ*, 339, 558
Auer, L. H., & Mihalas, D. 1969, *ApJ*, 158, 641
—, 1970, *ApJ*, 160, 233
—, 1972, *ApJS*, 24, 193
Bromm, V., Kudritzki, R. P., & Loeb, A. 2001, *ApJ*, 552, 464
Bromm, V., & Larson, R. B. 2004, *ARA&A*, 42, 79
Bromm, V., Yoshida, N., Hernquist, L., & McKee, C. F. 2009, *Nature*, 459, 49
Castor, J. I., Abbott, D. C., & Klein, R. I. 1975, *ApJ*, 195, 157
Gruschinske, J., & Kudritzki, R. P. 1979, *A&A*, 77, 341
Hauschildt, P. H., Baron, E., & Allard, F. 1997, *ApJ*, 483, 390
Hillier, D. J., & Miller, D. L. 1998, *ApJ*, 496, 407
Hirschi, R. 2007, *A&A*, 461, 571
Hubeny, I. 1988, *Computer Physics Communications*, 52, 103
Hubeny, I., & Lanz, T. 1995, *ApJ*, 439, 875
Johnson, J. L., Greif, T. H., & Bromm, V. 2008, in *IAU Symposium*, Vol. 250, *Massive Stars as Cosmic Engines*, ed. F. Bresolin, P. A. Crowther, & J. Puls, 471
Klapp, J. 1983, *Ap&SS*, 93, 313
Krtićka, J., & Kubát, J. 2004, *A&A*, 417, 1003
—, 2006, *A&A*, 446, 1039
—, 2009, *A&A*, 493, 585
Krtićka, J., Owocki, S. P., Kubát, J., Galloway, R. K., & Brown, J. C. 2003, *A&A*, 402, 713
Krtićka, J., Votruba, V., & Kubát, J. 2010, *A&A*, 516, A100
Kubát, J. 1994, *A&A*, 287, 179
—, 1995, *A&A*, 299, 803
—, 1996, *A&A*, 305, 255
—, 1997a, *A&A*, 323, 524
—, 1997b, *A&A*, 326, 277
—, 1997c, *A&A*, 324, 1020
—, 1999, *NewA*, 4, 157
—, 2001, *A&A*, 366, 210
Kubát, J. 2003, in *IAU Symposium*, Vol. 210, *Modelling of Stellar Atmospheres*, ed. N. Piskunov, W. W. Weiss, & D. F. Gray (Astronomical Society of Pacific), A8
Kubát, J., Puls, J., & Pauldrach, A. W. A. 1999, *A&A*, 341, 587
Kudritzki, R. P. 1973, *A&A*, 28, 103
—, 1976, *A&A*, 52, 11
—, 2002, *ApJ*, 577, 389
Lanz, T., & Hubeny, I. 2007, *ApJS*, 169, 83
Marigo, P., Girardi, L., Chiosi, C., & Wood, P. R. 2001, *A&A*, 371, 152
Mihalas, D. 1978, *Stellar Atmospheres*, 2nd ed. (W. H. Freeman & Co., San Francisco)
Mihalas, D., & Auer, L. H. 1970, *ApJ*, 160, 1161
Pauldrach, A. W. A. 2003, *Rev. Modern Astron.*, 16, 133
Puls, J., Urbaneja, M. A., Venero, R., et al. 2005, *A&A*, 435, 669
Santolaya-Rey, A. E., Puls, J., & Herrero, A. 1997, *A&A*, 323, 488
Schaerer, D. 2002, *A&A*, 382, 28
—, 2003, *A&A*, 397, 527
Tumlinson, J., & Shull, J. M. 2000, *ApJ*, 528, L65
Tumlinson, J., Shull, J. M., & Venkatesan, A. 2003, *ApJ*, 584, 608
Unsöld, A. 1955, *Physik der Sternatmosphären* (Springer Verlag, Berlin)
Venkatesan, A., & Truran, J. W. 2003, *ApJ*, 594, L1
Venkatesan, A., Tumlinson, J., & Shull, J. M. 2003, *ApJ*, 584, 621
Werner, K., Deetjen, J. L., Dreizler, S., et al. 2003, in *Astronomical Society of the Pacific Conference Series*, Vol. 288, *Stellar Atmosphere Modeling*, ed. I. Hubeny, D. Mihalas, & K. Werner, 31
Yoon, S.-C., & Langer, N. 2005, *A&A*, 443, 643
Yoon, S.-C., Langer, N., & Norman, C. 2006, *A&A*, 460, 199

APPENDIX

A. TEMPERATURE STRUCTURE OF CALCULATED MODEL ATMOSPHERES

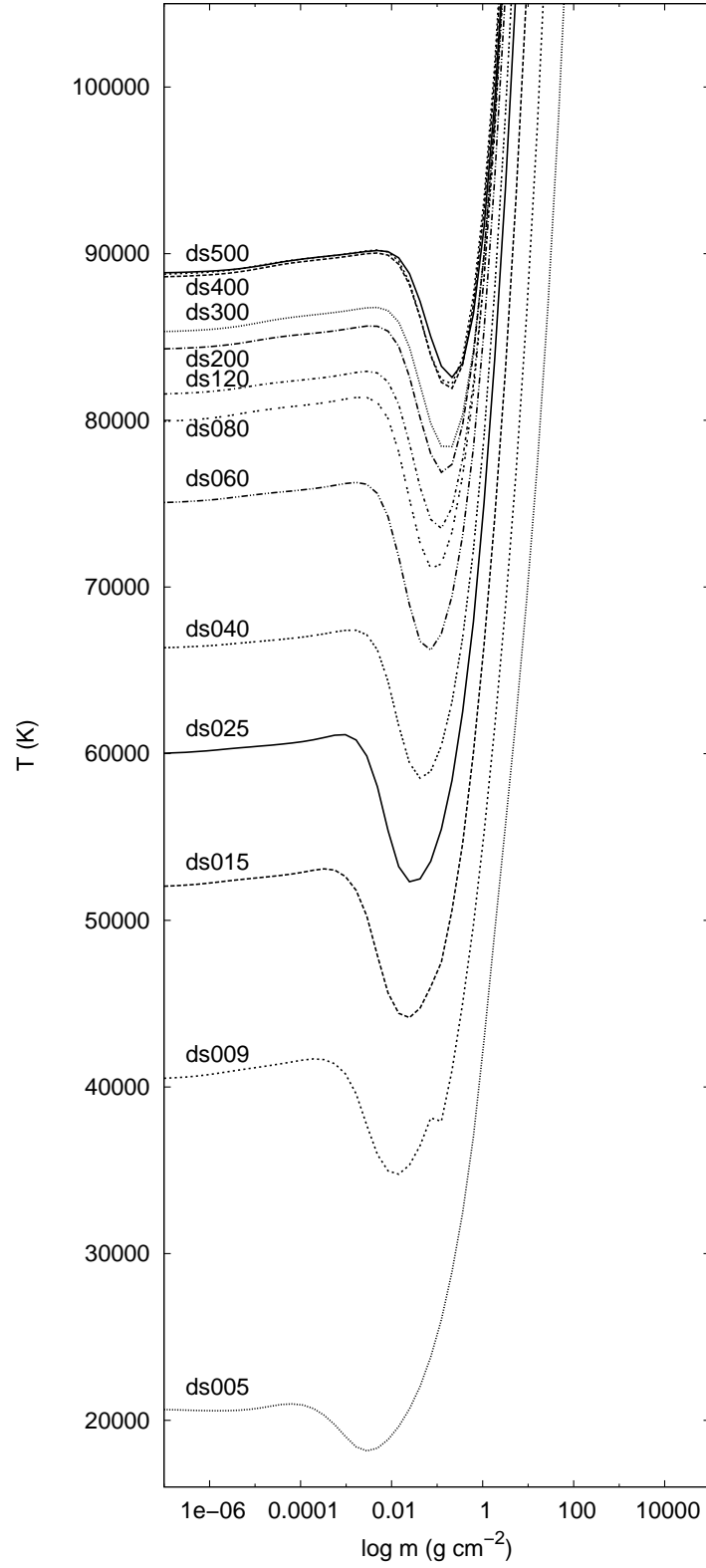


FIG. A1.— Run of temperature in NLTE model atmospheres of first stars with parameters after Schaerer (2002) listed in Table 1 (labels correspond to the first column of the table). The independent variable m is the column mass-depth (see Eq. 1).

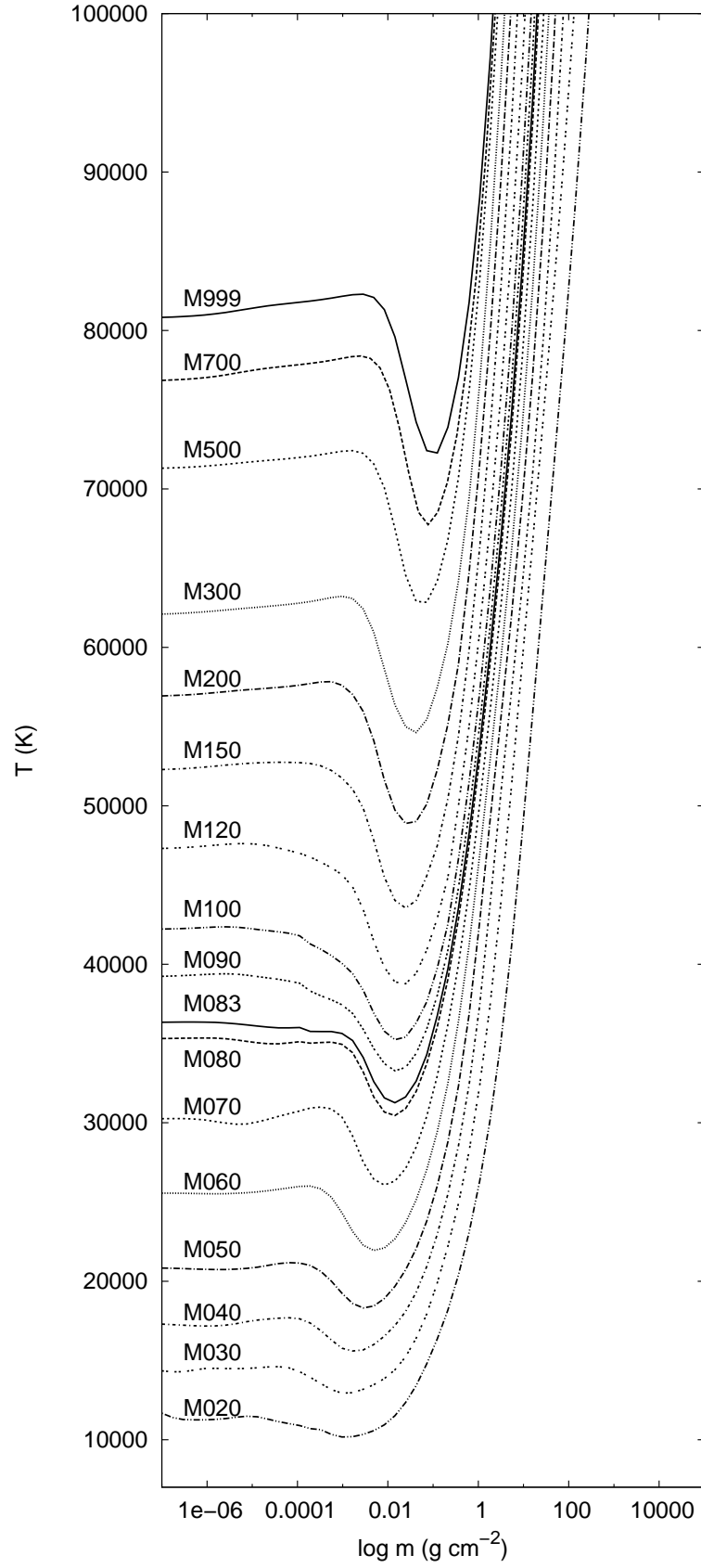


FIG. A2.— Run of temperature in NLTE model atmospheres of ZAMS first stars with stellar parameters after Marigo et al. (2001). Individual labels Mxxx correspond to to the first column of the Table 2. The independent variable m is the column mass-depth (see Eq. 1).

TABLE B1
MODEL ATMOSPHERE PARAMETERS AND AND STELLAR IONIZING PHOTON FLUXES Q_i FOR SELECTED MODEL ATMOSPHERES FROM THE
EVOLUTIONARY SEQUENCE FOR $100M_{\odot}$ FOR PARAMETERS FROM MARIGO ET AL. (2001).

age [years]	R_* [R_{\odot}]	M_* [M_{\odot}]	L [L_{\odot}]	T_{eff} [K]	$\log g$	$Q(\text{H I})$	$Q(\text{He I})$ [photons $\cdot \text{s}^{-1}$]	$Q(\text{He II})$
0.	4.23	100	$1.282 \cdot 10^6$	94400	5.185	$6.74 \cdot 10^{48}$	$4.18 \cdot 10^{48}$	$1.74 \cdot 10^{48}$
$3.781 \cdot 10^4$	4.43	100	$1.294 \cdot 10^6$	92470	5.145	$6.85 \cdot 10^{48}$	$4.20 \cdot 10^{48}$	$1.72 \cdot 10^{48}$
$1.330 \cdot 10^5$	4.54	100	$1.313 \cdot 10^6$	91620	5.123	$6.97 \cdot 10^{48}$	$4.25 \cdot 10^{48}$	$1.72 \cdot 10^{48}$
$2.571 \cdot 10^5$	4.69	100	$1.337 \cdot 10^6$	90570	5.095	$7.13 \cdot 10^{48}$	$4.31 \cdot 10^{48}$	$1.73 \cdot 10^{48}$
$3.966 \cdot 10^5$	4.83	100	$1.365 \cdot 10^6$	89740	5.070	$7.30 \cdot 10^{48}$	$4.39 \cdot 10^{48}$	$1.74 \cdot 10^{48}$
$5.232 \cdot 10^5$	4.96	100	$1.390 \cdot 10^6$	88920	5.046	$7.44 \cdot 10^{48}$	$4.49 \cdot 10^{48}$	$1.76 \cdot 10^{48}$
$7.771 \cdot 10^5$	5.28	100	$1.445 \cdot 10^6$	87100	4.993	$7.79 \cdot 10^{48}$	$4.59 \cdot 10^{48}$	$1.77 \cdot 10^{48}$
$1.001 \cdot 10^6$	5.57	100	$1.496 \cdot 10^6$	85500	4.946	$8.07 \cdot 10^{48}$	$4.69 \cdot 10^{48}$	$1.77 \cdot 10^{48}$
$1.201 \cdot 10^6$	5.91	100	$1.549 \cdot 10^6$	83750	4.895	$8.40 \cdot 10^{48}$	$4.80 \cdot 10^{48}$	$1.78 \cdot 10^{48}$
$1.375 \cdot 10^6$	6.27	100	$1.592 \cdot 10^6$	81840	4.843	$8.69 \cdot 10^{48}$	$4.88 \cdot 10^{48}$	$1.76 \cdot 10^{48}$
$1.589 \cdot 10^6$	6.81	100	$1.652 \cdot 10^6$	79250	4.771	$9.07 \cdot 10^{48}$	$4.96 \cdot 10^{48}$	$1.73 \cdot 10^{48}$
$1.647 \cdot 10^6$	7.01	100	$1.671 \cdot 10^6$	78340	4.746	$9.18 \cdot 10^{48}$	$4.98 \cdot 10^{48}$	$1.72 \cdot 10^{48}$
$1.701 \cdot 10^6$	7.18	100	$1.687 \cdot 10^6$	77620	4.726	$9.40 \cdot 10^{48}$	$5.31 \cdot 10^{48}$	$1.62 \cdot 10^{48}$
$1.753 \cdot 10^6$	7.34	100	$1.702 \cdot 10^6$	76910	4.706	$9.49 \cdot 10^{48}$	$5.33 \cdot 10^{48}$	$1.62 \cdot 10^{48}$
$1.802 \cdot 10^6$	7.55	100	$1.718 \cdot 10^6$	76030	4.682	$9.57 \cdot 10^{48}$	$5.34 \cdot 10^{48}$	$1.62 \cdot 10^{48}$
$1.893 \cdot 10^6$	7.94	100	$1.745 \cdot 10^6$	74470	4.639	$9.72 \cdot 10^{48}$	$5.35 \cdot 10^{48}$	$1.60 \cdot 10^{48}$
$1.941 \cdot 10^6$	8.18	100	$1.773 \cdot 10^6$	73620	4.612	$9.86 \cdot 10^{48}$	$5.38 \cdot 10^{48}$	$1.60 \cdot 10^{48}$
$2.018 \cdot 10^6$	8.57	100	$1.791 \cdot 10^6$	72110	4.572	$1.00 \cdot 10^{49}$	$5.03 \cdot 10^{48}$	$1.53 \cdot 10^{48}$
$2.093 \cdot 10^6$	9.03	100	$1.816 \cdot 10^6$	70470	4.526	$1.01 \cdot 10^{49}$	$5.33 \cdot 10^{48}$	$1.55 \cdot 10^{48}$
$2.188 \cdot 10^6$	9.72	100	$1.849 \cdot 10^6$	68230	4.462	$1.03 \cdot 10^{49}$	$5.30 \cdot 10^{48}$	$1.47 \cdot 10^{48}$
$2.319 \cdot 10^6$	11.0	100	$1.897 \cdot 10^6$	64560	4.355	$1.05 \cdot 10^{49}$	$5.17 \cdot 10^{48}$	$1.41 \cdot 10^{48}$
$2.408 \cdot 10^6$	12.1	100	$1.932 \cdot 10^6$	61940	4.275	$1.06 \cdot 10^{49}$	$5.06 \cdot 10^{48}$	$1.35 \cdot 10^{48}$
$2.500 \cdot 10^6$	13.7	100	$1.968 \cdot 10^6$	58480	4.167	$1.07 \cdot 10^{49}$	$4.83 \cdot 10^{48}$	$1.21 \cdot 10^{48}$
$2.547 \cdot 10^6$	14.6	100	$1.986 \cdot 10^6$	56620	4.107	$1.07 \cdot 10^{49}$	$4.67 \cdot 10^{48}$	$1.15 \cdot 10^{48}$
$2.590 \cdot 10^6$	15.7	100	$2.004 \cdot 10^6$	54830	4.047	$1.07 \cdot 10^{49}$	$4.51 \cdot 10^{48}$	$1.10 \cdot 10^{48}$
$2.603 \cdot 10^6$	16.1	100	$2.009 \cdot 10^6$	54200	4.026	$1.07 \cdot 10^{49}$	$4.45 \cdot 10^{48}$	$1.06 \cdot 10^{48}$
$2.628 \cdot 10^6$	16.8	100	$2.023 \cdot 10^6$	53090	3.987	$1.07 \cdot 10^{49}$	$4.35 \cdot 10^{48}$	$9.85 \cdot 10^{47}$
$2.654 \cdot 10^6$	17.6	100	$2.032 \cdot 10^6$	51880	3.945	$1.06 \cdot 10^{49}$	$4.22 \cdot 10^{48}$	$9.74 \cdot 10^{47}$
$2.701 \cdot 10^6$	19.6	100	$2.056 \cdot 10^6$	49320	3.852	$1.03 \cdot 10^{49}$	$3.61 \cdot 10^{48}$	$5.67 \cdot 10^{47}$
$2.755 \cdot 10^6$	22.5	100	$2.080 \cdot 10^6$	46240	3.735	$1.03 \cdot 10^{49}$	$3.29 \cdot 10^{48}$	$4.70 \cdot 10^{47}$
$2.805 \cdot 10^6$	26.0	100	$2.109 \cdot 10^6$	43150	3.609	$9.86 \cdot 10^{48}$	$2.74 \cdot 10^{48}$	$3.41 \cdot 10^{47}$
$2.812 \cdot 10^6$	26.6	100	$2.109 \cdot 10^6$	42660	3.589	$9.81 \cdot 10^{48}$	$2.68 \cdot 10^{48}$	$3.28 \cdot 10^{47}$
$2.820 \cdot 10^6$	27.2	100	$2.113 \cdot 10^6$	42170	3.568	$9.75 \cdot 10^{48}$	$2.62 \cdot 10^{48}$	$3.17 \cdot 10^{47}$
$2.827 \cdot 10^6$	27.9	100	$2.118 \cdot 10^6$	41690	3.547	$9.70 \cdot 10^{48}$	$2.55 \cdot 10^{48}$	$3.03 \cdot 10^{47}$
$2.834 \cdot 10^6$	28.6	100	$2.123 \cdot 10^6$	41210	3.526	$9.64 \cdot 10^{48}$	$2.49 \cdot 10^{48}$	$2.91 \cdot 10^{47}$
$2.855 \cdot 10^6$	30.7	100	$2.138 \cdot 10^6$	39810	3.463	$9.45 \cdot 10^{48}$	$2.28 \cdot 10^{48}$	$2.54 \cdot 10^{47}$
$2.863 \cdot 10^6$	31.5	100	$2.148 \cdot 10^6$	39350	3.441	$9.41 \cdot 10^{48}$	$2.22 \cdot 10^{48}$	$2.44 \cdot 10^{47}$
$2.870 \cdot 10^6$	30.0	100	$2.193 \cdot 10^6$	40550	3.484	$9.90 \cdot 10^{48}$	$2.46 \cdot 10^{48}$	$2.75 \cdot 10^{47}$
$2.870 \cdot 10^6$	29.4	100	$2.203 \cdot 10^6$	41020	3.502	$1.01 \cdot 10^{49}$	$2.56 \cdot 10^{48}$	$2.90 \cdot 10^{47}$
$2.871 \cdot 10^6$	28.9	100	$2.213 \cdot 10^6$	41400	3.516	$1.02 \cdot 10^{49}$	$2.63 \cdot 10^{48}$	$3.02 \cdot 10^{47}$
$2.873 \cdot 10^6$	29.6	100	$2.218 \cdot 10^6$	40930	3.495	$1.01 \cdot 10^{49}$	$2.56 \cdot 10^{48}$	$2.91 \cdot 10^{47}$
$2.874 \cdot 10^6$	30.3	100	$2.218 \cdot 10^6$	40460	3.475	$1.00 \cdot 10^{49}$	$2.47 \cdot 10^{48}$	$2.77 \cdot 10^{47}$
$2.889 \cdot 10^6$	37.4	100	$2.239 \cdot 10^6$	36470	3.291	$9.09 \cdot 10^{48}$	$1.74 \cdot 10^{48}$	$1.55 \cdot 10^{47}$
$2.900 \cdot 10^6$	42.5	100	$2.249 \cdot 10^6$	34280	3.181	$8.40 \cdot 10^{48}$	$1.35 \cdot 10^{48}$	$1.05 \cdot 10^{47}$
$2.911 \cdot 10^6$	48.0	100	$2.259 \cdot 10^6$	32280	3.075	$7.67 \cdot 10^{48}$	$1.01 \cdot 10^{48}$	$6.74 \cdot 10^{46}$
$2.920 \cdot 10^6$	53.4	100	$2.265 \cdot 10^6$	30620	2.982	$6.93 \cdot 10^{48}$	$7.31 \cdot 10^{47}$	$4.25 \cdot 10^{46}$
$2.925 \cdot 10^6$	56.4	100	$2.280 \cdot 10^6$	29850	2.935	$6.58 \cdot 10^{48}$	$6.18 \cdot 10^{47}$	$3.35 \cdot 10^{46}$
$2.975 \cdot 10^6$	125.	100	$2.311 \cdot 10^6$	20090	2.241	$5.86 \cdot 10^{47}$	$6.01 \cdot 10^{42}$	$3.15 \cdot 10^{39}$
$3.014 \cdot 10^6$	510.	100	$2.327 \cdot 10^6$	9977	1.022	$3.86 \cdot 10^{42}$	$1.05 \cdot 10^{36}$	$1.32 \cdot 10^{27}$

B. IONIZING FLUXES DURING FIRST STAR EVOLUTION

TABLE B2
THE SAME AS TABLE B1 BUT FOR $50M_{\odot}$.

age	R_*	M_*	L	T_{eff}	$\log g$	$Q(\text{H I})$	$Q(\text{He I})$	$Q(\text{He II})$
[years]	$[R_{\odot}]$	$[M_{\odot}]$	$[L_{\odot}]$	[K]			[photons $\cdot \text{s}^{-1}$]	
0	2.82	50	$3.597 \cdot 10^5$	84140	5.236	$2.01 \cdot 10^{48}$	$1.16 \cdot 10^{48}$	$3.80 \cdot 10^{47}$
$9.203 \cdot 10^4$	2.99	50	$3.664 \cdot 10^5$	82035	5.183	$2.06 \cdot 10^{48}$	$1.17 \cdot 10^{48}$	$3.79 \cdot 10^{47}$
$2.545 \cdot 10^5$	3.08	50	$3.741 \cdot 10^5$	81280	5.159	$2.09 \cdot 10^{48}$	$1.18 \cdot 10^{48}$	$3.82 \cdot 10^{47}$
$4.606 \cdot 10^5$	3.17	50	$3.846 \cdot 10^5$	80720	5.135	$2.18 \cdot 10^{48}$	$1.21 \cdot 10^{48}$	$3.93 \cdot 10^{47}$
$6.683 \cdot 10^5$	3.27	50	$3.954 \cdot 10^5$	79980	5.107	$2.21 \cdot 10^{48}$	$1.23 \cdot 10^{48}$	$3.99 \cdot 10^{47}$
$8.760 \cdot 10^5$	3.38	50	$4.064 \cdot 10^5$	79250	5.079	$2.27 \cdot 10^{48}$	$1.26 \cdot 10^{48}$	$4.06 \cdot 10^{47}$
$1.063 \cdot 10^6$	3.47	50	$4.178 \cdot 10^5$	78700	5.055	$2.34 \cdot 10^{48}$	$1.29 \cdot 10^{48}$	$4.00 \cdot 10^{47}$
$1.432 \cdot 10^6$	3.71	50	$4.416 \cdot 10^5$	77270	4.999	$2.48 \cdot 10^{48}$	$1.34 \cdot 10^{48}$	$4.07 \cdot 10^{47}$
$2.024 \cdot 10^6$	4.18	50	$4.842 \cdot 10^5$	74470	4.895	$2.72 \cdot 10^{48}$	$1.44 \cdot 10^{48}$	$4.32 \cdot 10^{47}$
$2.359 \cdot 10^6$	4.56	50	$5.129 \cdot 10^5$	72280	4.818	$2.87 \cdot 10^{48}$	$1.47 \cdot 10^{48}$	$4.23 \cdot 10^{47}$
$2.642 \cdot 10^6$	4.99	50	$5.383 \cdot 10^5$	69980	4.741	$3.00 \cdot 10^{48}$	$1.50 \cdot 10^{48}$	$4.21 \cdot 10^{47}$
$2.957 \cdot 10^6$	5.63	50	$5.702 \cdot 10^5$	66830	4.636	$3.16 \cdot 10^{48}$	$1.53 \cdot 10^{48}$	$4.18 \cdot 10^{47}$
$3.289 \cdot 10^6$	6.68	50	$6.095 \cdot 10^5$	62370	4.487	$3.33 \cdot 10^{48}$	$1.51 \cdot 10^{48}$	$3.89 \cdot 10^{47}$
$3.584 \cdot 10^6$	8.20	50	$6.471 \cdot 10^5$	57150	4.309	$3.44 \cdot 10^{48}$	$1.43 \cdot 10^{48}$	$3.56 \cdot 10^{47}$
$3.613 \cdot 10^6$	8.42	50	$6.516 \cdot 10^5$	56490	4.286	$3.45 \cdot 10^{48}$	$1.42 \cdot 10^{48}$	$3.48 \cdot 10^{47}$
$3.640 \cdot 10^6$	8.65	50	$6.561 \cdot 10^5$	55850	4.263	$3.46 \cdot 10^{48}$	$1.40 \cdot 10^{48}$	$3.39 \cdot 10^{47}$
$3.669 \cdot 10^6$	8.87	50	$6.592 \cdot 10^5$	55210	4.241	$3.46 \cdot 10^{48}$	$1.39 \cdot 10^{48}$	$3.33 \cdot 10^{47}$
$3.866 \cdot 10^6$	11.1	50	$6.949 \cdot 10^5$	50000	4.046	$3.48 \cdot 10^{48}$	$1.20 \cdot 10^{48}$	$2.24 \cdot 10^{47}$
$3.946 \cdot 10^6$	12.4	50	$7.046 \cdot 10^5$	47530	3.952	$3.41 \cdot 10^{48}$	$1.09 \cdot 10^{48}$	$1.95 \cdot 10^{47}$
$4.021 \cdot 10^6$	13.6	50	$7.228 \cdot 10^5$	45600	3.869	$3.39 \cdot 10^{48}$	$1.02 \cdot 10^{48}$	$1.74 \cdot 10^{47}$
$4.031 \cdot 10^6$	13.4	50	$7.311 \cdot 10^5$	46020	3.880	$3.45 \cdot 10^{48}$	$1.05 \cdot 10^{48}$	$1.82 \cdot 10^{47}$
$4.032 \cdot 10^6$	13.2	50	$7.362 \cdot 10^5$	46560	3.897	$3.51 \cdot 10^{48}$	$1.09 \cdot 10^{48}$	$1.90 \cdot 10^{47}$
$4.039 \cdot 10^6$	12.6	50	$7.621 \cdot 10^5$	48080	3.938	$3.74 \cdot 10^{48}$	$1.21 \cdot 10^{48}$	$2.18 \cdot 10^{47}$
$4.047 \cdot 10^6$	12.8	50	$7.656 \cdot 10^5$	47640	3.920	$3.73 \cdot 10^{48}$	$1.19 \cdot 10^{48}$	$2.13 \cdot 10^{47}$
$4.064 \cdot 10^6$	13.1	50	$7.673 \cdot 10^5$	47100	3.899	$3.71 \cdot 10^{48}$	$1.17 \cdot 10^{48}$	$2.06 \cdot 10^{47}$
$4.075 \cdot 10^6$	13.5	50	$7.691 \cdot 10^5$	46560	3.878	$3.68 \cdot 10^{48}$	$1.14 \cdot 10^{48}$	$1.99 \cdot 10^{47}$
$4.084 \cdot 10^6$	13.8	50	$7.709 \cdot 10^5$	46020	3.857	$3.66 \cdot 10^{48}$	$1.11 \cdot 10^{48}$	$1.92 \cdot 10^{47}$
$4.092 \cdot 10^6$	14.1	50	$7.727 \cdot 10^5$	45500	3.836	$3.63 \cdot 10^{48}$	$1.09 \cdot 10^{48}$	$1.86 \cdot 10^{47}$
$4.099 \cdot 10^6$	14.5	50	$7.727 \cdot 10^5$	44980	3.816	$3.60 \cdot 10^{48}$	$1.06 \cdot 10^{48}$	$1.78 \cdot 10^{47}$
$4.106 \cdot 10^6$	14.8	50	$7.745 \cdot 10^5$	44560	3.799	$3.58 \cdot 10^{48}$	$1.04 \cdot 10^{48}$	$1.73 \cdot 10^{47}$
$4.112 \cdot 10^6$	15.1	50	$7.762 \cdot 10^5$	44050	3.778	$3.55 \cdot 10^{48}$	$1.01 \cdot 10^{48}$	$1.67 \cdot 10^{47}$
$4.118 \cdot 10^6$	15.5	50	$7.780 \cdot 10^5$	43550	3.757	$3.52 \cdot 10^{48}$	$9.83 \cdot 10^{47}$	$1.61 \cdot 10^{47}$
$4.150 \cdot 10^6$	17.8	50	$7.852 \cdot 10^5$	40740	3.637	$3.31 \cdot 10^{48}$	$8.25 \cdot 10^{47}$	$1.26 \cdot 10^{47}$
$4.159 \cdot 10^6$	18.6	50	$7.870 \cdot 10^5$	39900	3.600	$3.23 \cdot 10^{48}$	$7.77 \cdot 10^{47}$	$1.16 \cdot 10^{47}$
$4.204 \cdot 10^6$	23.6	50	$7.980 \cdot 10^5$	35480	3.390	$2.73 \cdot 10^{48}$	$4.33 \cdot 10^{47}$	$3.37 \cdot 10^{46}$
$4.220 \cdot 10^6$	26.1	50	$8.017 \cdot 10^5$	33810	3.304	$2.48 \cdot 10^{48}$	$3.14 \cdot 10^{47}$	$2.11 \cdot 10^{46}$
$4.256 \cdot 10^6$	33.7	50	$8.139 \cdot 10^5$	29850	3.081	$1.75 \cdot 10^{48}$	$9.08 \cdot 10^{46}$	$3.89 \cdot 10^{45}$
$4.328 \cdot 10^6$	72.0	50	$8.355 \cdot 10^5$	20560	2.422	$6.34 \cdot 10^{45}$	$2.04 \cdot 10^{40}$	$3.49 \cdot 10^{35}$
$4.366 \cdot 10^6$	303.	50	$8.502 \cdot 10^5$	10070	1.174	$1.29 \cdot 10^{41}$	$5.33 \cdot 10^{35}$	$2.07 \cdot 10^{26}$

TABLE B3
THE SAME AS TABLE B1 BUT FOR $20M_{\odot}$.

age	R_*	M_*	L	T_{eff}	$\log g$	$Q(\text{H I})$	$Q(\text{He I})$	$Q(\text{He II})$
[years]	[R_{\odot}]	[M_{\odot}]	[L_{\odot}]	[K]			[photons $\cdot \text{s}^{-1}$]	
0	1.65	20	$4.456 \cdot 10^4$	65310	5.305	$2.40 \cdot 10^{47}$	$1.27 \cdot 10^{47}$	$3.24 \cdot 10^{46}$
$2.720 \cdot 10^5$	1.73	20	$4.613 \cdot 10^4$	64120	5.258	$2.46 \cdot 10^{47}$	$1.29 \cdot 10^{47}$	$3.24 \cdot 10^{46}$
$1.581 \cdot 10^6$	1.90	20	$5.093 \cdot 10^4$	62800	5.179	$2.69 \cdot 10^{47}$	$1.39 \cdot 10^{47}$	$3.44 \cdot 10^{46}$
$3.164 \cdot 10^6$	2.15	20	$5.834 \cdot 10^4$	61090	5.072	$3.05 \cdot 10^{47}$	$1.53 \cdot 10^{47}$	$3.71 \cdot 10^{46}$
$4.726 \cdot 10^6$	2.52	20	$6.776 \cdot 10^4$	58610	4.935	$3.52 \cdot 10^{47}$	$1.70 \cdot 10^{47}$	$3.91 \cdot 10^{46}$
$6.497 \cdot 10^6$	3.31	20	$8.317 \cdot 10^4$	53830	4.698	$4.13 \cdot 10^{47}$	$1.80 \cdot 10^{47}$	$3.49 \cdot 10^{46}$
$7.004 \cdot 10^6$	3.73	20	$8.913 \cdot 10^4$	51640	4.596	$4.30 \cdot 10^{47}$	$1.79 \cdot 10^{47}$	$3.32 \cdot 10^{46}$
$7.306 \cdot 10^6$	4.10	20	$9.480 \cdot 10^4$	50000	4.513	$4.45 \cdot 10^{47}$	$1.79 \cdot 10^{47}$	$3.23 \cdot 10^{46}$
$7.630 \cdot 10^6$	4.54	20	$9.772 \cdot 10^4$	47860	4.424	$4.40 \cdot 10^{47}$	$1.68 \cdot 10^{47}$	$2.92 \cdot 10^{46}$
$8.012 \cdot 10^6$	5.34	20	$1.042 \cdot 10^5$	44870	4.284	$4.33 \cdot 10^{47}$	$1.52 \cdot 10^{47}$	$2.49 \cdot 10^{46}$
$8.078 \cdot 10^6$	5.50	20	$1.057 \cdot 10^5$	44360	4.258	$4.32 \cdot 10^{47}$	$1.49 \cdot 10^{47}$	$2.42 \cdot 10^{46}$
$8.151 \cdot 10^6$	5.65	20	$1.074 \cdot 10^5$	43950	4.235	$4.34 \cdot 10^{47}$	$1.48 \cdot 10^{47}$	$2.38 \cdot 10^{46}$
$8.202 \cdot 10^6$	5.60	20	$1.096 \cdot 10^5$	44360	4.242	$4.50 \cdot 10^{47}$	$1.55 \cdot 10^{47}$	$2.51 \cdot 10^{46}$
$8.212 \cdot 10^6$	5.46	20	$1.132 \cdot 10^5$	45290	4.264	$4.78 \cdot 10^{47}$	$1.69 \cdot 10^{47}$	$2.78 \cdot 10^{46}$
$8.216 \cdot 10^6$	5.28	20	$1.191 \cdot 10^5$	46660	4.294	$5.23 \cdot 10^{47}$	$1.92 \cdot 10^{47}$	$3.22 \cdot 10^{46}$
$8.235 \cdot 10^6$	5.09	20	$1.216 \cdot 10^5$	47750	4.325	$5.49 \cdot 10^{47}$	$2.06 \cdot 10^{47}$	$3.53 \cdot 10^{46}$
$8.267 \cdot 10^6$	4.94	20	$1.202 \cdot 10^5$	48300	4.350	$5.49 \cdot 10^{47}$	$2.09 \cdot 10^{47}$	$3.62 \cdot 10^{46}$
$8.405 \cdot 10^6$	5.36	20	$1.225 \cdot 10^5$	46770	4.286	$5.40 \cdot 10^{47}$	$1.98 \cdot 10^{47}$	$3.33 \cdot 10^{46}$
$8.506 \cdot 10^6$	5.85	20	$1.250 \cdot 10^5$	44870	4.205	$5.25 \cdot 10^{47}$	$1.83 \cdot 10^{47}$	$2.95 \cdot 10^{46}$
$8.607 \cdot 10^6$	6.57	20	$1.279 \cdot 10^5$	42560	4.103	$4.99 \cdot 10^{47}$	$1.61 \cdot 10^{47}$	$2.49 \cdot 10^{46}$
$8.697 \cdot 10^6$	7.44	20	$1.312 \cdot 10^5$	40270	3.996	$4.65 \cdot 10^{47}$	$1.38 \cdot 10^{47}$	$2.03 \cdot 10^{46}$
$8.744 \cdot 10^6$	8.00	20	$1.334 \cdot 10^5$	38990	3.933	$4.47 \cdot 10^{47}$	$1.27 \cdot 10^{47}$	$1.82 \cdot 10^{46}$
$8.774 \cdot 10^6$	8.58	20	$1.349 \cdot 10^5$	37760	3.872	$4.20 \cdot 10^{47}$	$1.13 \cdot 10^{47}$	$1.58 \cdot 10^{46}$
$8.786 \cdot 10^6$	8.97	20	$1.358 \cdot 10^5$	36980	3.833	$4.02 \cdot 10^{47}$	$1.04 \cdot 10^{47}$	$1.43 \cdot 10^{46}$
$8.790 \cdot 10^6$	9.18	20	$1.358 \cdot 10^5$	36560	3.813	$3.87 \cdot 10^{47}$	$5.84 \cdot 10^{46}$	$5.18 \cdot 10^{45}$
$8.795 \cdot 10^6$	10.5	20	$1.312 \cdot 10^5$	33960	3.700	$2.81 \cdot 10^{47}$	$1.97 \cdot 10^{46}$	$1.25 \cdot 10^{45}$
$8.800 \cdot 10^6$	13.8	20	$1.318 \cdot 10^5$	29580	3.458	$1.11 \cdot 10^{47}$	$1.68 \cdot 10^{44}$	$1.58 \cdot 10^{41}$
$8.805 \cdot 10^6$	19.9	20	$1.297 \cdot 10^5$	24550	3.141	$5.78 \cdot 10^{45}$	$7.50 \cdot 10^{41}$	$1.91 \cdot 10^{38}$

TABLE B4
THE SAME AS TABLE B1 BUT FOR $10M_{\odot}$.

age	R_*	M_*	L	T_{eff}	$\log g$	$Q(\text{H I})$	$Q(\text{He I})$	$Q(\text{He II})$
[years]	[R_{\odot}]	[M_{\odot}]	[L_{\odot}]	[K]			[photons $\cdot \text{s}^{-1}$]	
0	1.37	10	$6.653 \cdot 10^3$	44460	5.162	$2.48 \cdot 10^{46}$	$8.36 \cdot 10^{45}$	$1.39 \cdot 10^{45}$
$4.445 \cdot 10^5$	1.38	10	$6.887 \cdot 10^3$	44770	5.159	$2.61 \cdot 10^{46}$	$8.94 \cdot 10^{45}$	$1.50 \cdot 10^{45}$
$3.584 \cdot 10^6$	1.39	10	$7.852 \cdot 10^3$	46020	5.150	$3.12 \cdot 10^{46}$	$1.13 \cdot 10^{46}$	$1.94 \cdot 10^{45}$
$5.616 \cdot 10^6$	1.41	10	$8.690 \cdot 10^3$	46990	5.142	$3.57 \cdot 10^{46}$	$1.34 \cdot 10^{46}$	$2.34 \cdot 10^{45}$
$8.502 \cdot 10^6$	1.47	10	$9.954 \cdot 10^3$	47530	5.103	$4.15 \cdot 10^{46}$	$1.59 \cdot 10^{46}$	$2.82 \cdot 10^{45}$
$1.068 \cdot 10^7$	1.62	10	$1.081 \cdot 10^4$	46240	5.019	$4.42 \cdot 10^{46}$	$1.63 \cdot 10^{46}$	$2.83 \cdot 10^{45}$
$1.296 \cdot 10^7$	1.83	10	$1.197 \cdot 10^4$	44560	4.911	$4.60 \cdot 10^{46}$	$1.62 \cdot 10^{46}$	$2.76 \cdot 10^{45}$
$1.493 \cdot 10^7$	2.13	10	$1.327 \cdot 10^4$	42460	4.782	$4.73 \cdot 10^{46}$	$1.56 \cdot 10^{46}$	$2.57 \cdot 10^{45}$
$1.658 \cdot 10^7$	2.52	10	$1.469 \cdot 10^4$	39990	4.634	$4.51 \cdot 10^{46}$	$1.34 \cdot 10^{46}$	$2.14 \cdot 10^{45}$
$1.725 \cdot 10^7$	2.76	10	$1.541 \cdot 10^4$	38720	4.557	$4.20 \cdot 10^{46}$	$1.13 \cdot 10^{46}$	$1.79 \cdot 10^{45}$
$1.746 \cdot 10^7$	2.84	10	$1.567 \cdot 10^4$	38280	4.530	$4.11 \cdot 10^{46}$	$1.09 \cdot 10^{46}$	$1.71 \cdot 10^{45}$
$1.769 \cdot 10^7$	2.92	10	$1.596 \cdot 10^4$	37930	4.506	$4.06 \cdot 10^{46}$	$1.06 \cdot 10^{46}$	$1.67 \cdot 10^{45}$
$1.778 \cdot 10^7$	2.95	10	$1.614 \cdot 10^4$	37840	4.497	$4.08 \cdot 10^{46}$	$1.05 \cdot 10^{46}$	$1.65 \cdot 10^{45}$
$1.791 \cdot 10^7$	2.93	10	$1.652 \cdot 10^4$	38190	4.503	$4.32 \cdot 10^{46}$	$1.14 \cdot 10^{46}$	$1.80 \cdot 10^{45}$
$1.794 \cdot 10^7$	2.89	10	$1.679 \cdot 10^4$	38640	4.516	$4.57 \cdot 10^{46}$	$1.24 \cdot 10^{46}$	$1.96 \cdot 10^{45}$
$1.795 \cdot 10^7$	2.87	10	$1.714 \cdot 10^4$	38990	4.523	$4.81 \cdot 10^{46}$	$1.34 \cdot 10^{46}$	$2.12 \cdot 10^{45}$
$1.795 \cdot 10^7$	2.84	10	$1.750 \cdot 10^4$	39350	4.530	$5.06 \cdot 10^{46}$	$1.44 \cdot 10^{46}$	$2.28 \cdot 10^{45}$
$1.796 \cdot 10^7$	2.82	10	$1.791 \cdot 10^4$	39720	4.536	$5.33 \cdot 10^{46}$	$1.56 \cdot 10^{46}$	$2.51 \cdot 10^{45}$
$1.796 \cdot 10^7$	2.80	10	$1.832 \cdot 10^4$	40090	4.542	$5.60 \cdot 10^{46}$	$1.67 \cdot 10^{46}$	$2.68 \cdot 10^{45}$
$1.796 \cdot 10^7$	2.79	10	$1.879 \cdot 10^4$	40460	4.547	$5.89 \cdot 10^{46}$	$1.79 \cdot 10^{46}$	$2.88 \cdot 10^{45}$
$1.804 \cdot 10^7$	2.74	10	$1.950 \cdot 10^4$	41210	4.563	$6.41 \cdot 10^{46}$	$2.02 \cdot 10^{46}$	$3.27 \cdot 10^{45}$
$1.810 \cdot 10^7$	2.68	10	$1.932 \cdot 10^4$	41590	4.583	$6.49 \cdot 10^{46}$	$2.07 \cdot 10^{46}$	$3.36 \cdot 10^{45}$
$1.825 \cdot 10^7$	2.61	10	$1.928 \cdot 10^4$	42070	4.604	$6.64 \cdot 10^{46}$	$2.16 \cdot 10^{46}$	$3.51 \cdot 10^{45}$
$1.829 \cdot 10^7$	2.61	10	$1.928 \cdot 10^4$	42070	4.604	$6.64 \cdot 10^{46}$	$2.16 \cdot 10^{46}$	$3.51 \cdot 10^{45}$
$1.862 \cdot 10^7$	2.68	10	$1.963 \cdot 10^4$	41690	4.580	$6.63 \cdot 10^{46}$	$2.13 \cdot 10^{46}$	$3.46 \cdot 10^{45}$
$1.878 \cdot 10^7$	2.75	10	$1.986 \cdot 10^4$	41300	4.559	$6.58 \cdot 10^{46}$	$2.07 \cdot 10^{46}$	$3.35 \cdot 10^{45}$
$1.888 \cdot 10^7$	2.83	10	$2.009 \cdot 10^4$	40830	4.534	$6.47 \cdot 10^{46}$	$2.00 \cdot 10^{46}$	$3.21 \cdot 10^{45}$
$1.899 \cdot 10^7$	2.91	10	$2.042 \cdot 10^4$	40460	4.511	$6.56 \cdot 10^{46}$	$2.01 \cdot 10^{46}$	$3.20 \cdot 10^{45}$
$1.909 \cdot 10^7$	2.98	10	$2.075 \cdot 10^4$	40090	4.488	$6.55 \cdot 10^{46}$	$1.99 \cdot 10^{46}$	$3.17 \cdot 10^{45}$
$1.919 \cdot 10^7$	3.06	10	$2.109 \cdot 10^4$	39720	4.465	$6.50 \cdot 10^{46}$	$1.94 \cdot 10^{46}$	$3.07 \cdot 10^{45}$
$1.927 \cdot 10^7$	3.16	10	$2.143 \cdot 10^4$	39260	4.438	$6.40 \cdot 10^{46}$	$1.87 \cdot 10^{46}$	$2.93 \cdot 10^{45}$
$1.938 \cdot 10^7$	3.93	10	$2.000 \cdot 10^4$	34590	4.248	$3.25 \cdot 10^{46}$	$1.43 \cdot 10^{45}$	$9.46 \cdot 10^{43}$
$1.940 \cdot 10^7$	5.25	10	$2.104 \cdot 10^4$	30340	3.998	$8.90 \cdot 10^{45}$	$1.08 \cdot 10^{43}$	$8.24 \cdot 10^{39}$
$1.943 \cdot 10^7$	11.4	10	$1.946 \cdot 10^4$	20180	3.324	$8.52 \cdot 10^{43}$	$1.04 \cdot 10^{39}$	$3.32 \cdot 10^{34}$
$1.943 \cdot 10^7$	12.3	10	$1.928 \cdot 10^4$	19360	3.256	$7.27 \cdot 10^{43}$	$9.12 \cdot 10^{38}$	$6.10 \cdot 10^{33}$
$1.943 \cdot 10^7$	15.9	10	$1.897 \cdot 10^4$	16980	3.035	$2.04 \cdot 10^{43}$	$1.75 \cdot 10^{40}$	$4.64 \cdot 10^{34}$